

Self-Calibration of CMB Polarization Experiments

Brian G. Keating¹, Meir Shimon², and Amit P.S. Yadav¹

¹*Center for Astrophysics and Space Sciences,
Department of Physics, University of California,
San Diego, 9500 Gilman Drive,
La Jolla, CA, 92093-0424*

²*School of Physics and Astronomy,
Tel Aviv University, Tel Aviv 69978, Israel*

(Dated: September 3, 2018)

Precision measurements of the polarization of the cosmic microwave background (CMB) radiation, especially experiments seeking to detect the odd-parity “B-modes”, have far-reaching implications for cosmology. To detect the B-modes generated during inflation the flux response and polarization angle of these experiments must be calibrated to exquisite precision. While suitable flux calibration sources abound, polarization angle calibrators are deficient in many respects. Man-made polarized sources are often not located in the antenna’s far-field, have spectral properties that are radically different from the CMB’s, are cumbersome to implement and may be inherently unstable over the (long) duration these searches require to detect the faint signature of the inflationary epoch. Astrophysical sources suffer from time, frequency and spatial variability, are not visible from all CMB observatories, and none are understood with sufficient accuracy to calibrate future CMB polarimeters seeking to probe inflationary energy scales of 10^{15} GeV. Furthermore, both man-made and astrophysical sources are often much brighter than the CMB B-mode signal and these bright sources can cause non-linearities in the detector’s response. Both man-made and astrophysical sources require dedicated observations which detract from the amount of integration time usable for detection of the inflationary B-modes. CMB TB and EB modes, expected to identically vanish in the standard cosmological model, can be used to calibrate CMB polarimeters. By enforcing the observed EB and TB power spectra to be consistent with zero, CMB polarimeters can be calibrated to levels not possible with man-made or astrophysical sources. All of this can be accomplished without any loss of observing time using a calibration source which is spectrally identical to the CMB B-modes. The calibration procedure outlined here can be used for any CMB polarimeter.

PACS numbers: 98.80.Cq, 04.50.-h

Introduction: Inflation is perhaps the most promising model of the early universe, resolving the Big Bang model’s flatness and horizon problems and providing seed perturbations for structure formation (see *e.g.*, [1] for review). Besides the density, or “scalar”, seed perturbations, inflationary cosmological models also predict “tensor” perturbations arising from a primordial gravitational wave background. Primordial scalar perturbations create only CMB E -modes, while primordial tensor perturbations generate both parity-even E -modes and parity-odd B -modes polarization [2–4]. The detection of primordial tensor B -modes in the CMB would confirm the existence of gravitational wave perturbations in the early universe. Numerous observational efforts are underway to detect the CMB’s B -mode since such a detection would establish the energy scale at which inflation occurred. The amplitude of primordial B -modes can be characterized by the tensor-to-scalar ratio, r . The most restrictive limit on r is currently $r < 0.18$ (95% confidence) [5], and the best direct limits on r from B -mode measurements is $r < 0.72$ (95% confidence) [6].

An impressive battery of CMB experiments have mapped the CMB’s intensity to near cosmic-variance-limited precision to $\ell \sim 3000$ [5, 7, 8]. However, the

measurement of the CMB’s E -mode polarization signal is considerably more challenging since it is 10 to 100 times smaller than the CMB’s temperature anisotropy. Compared to these signals the B -mode polarization from inflationary gravitational waves is even more challenging – current upper limits correspond to B -mode fluctuations less than 10% of the E -modes. Calibration accuracy required by a given instrument to constrain or detect the minute B -mode signal is well-discussed in the literature [9]. Calibration is accomplished either using hardware calibrators, located in the near field of the instrument [10–13], or by measurements of polarized astrophysical sources, *e.g.* the Moon, Tau A, Cen A, 3C 273, or the galactic plane [14–17]. Neither hardware polarization calibrators nor astrophysical sources can achieve better than $\simeq 1^\circ$ precision on the polarization angle calibration. It is hard, if not impossible, to do better, yet a precision of 1° is insufficient for detecting $r = 0.025$ to 0.01 [9] – the goal of future polarimeters. Rather, it has been shown [18] that for $r = 0.01$ to be biased by $\lesssim 0.1\sigma_r$ (where σ_r is the nominal statistical uncertainty on the inferred value of r), the uncertainty in pixel rotation cannot exceed $4'$ even for a nearly ideal CMB experiment. Even relaxing this requirement, by

allowing a bias on r as large as $\simeq 1\sigma_r$, only permits a miscalibration level of $\lesssim 12'$.

Miscalibration of the instrument's polarization angle (pixel rotation) mixes polarization modes, leaking E - into B -modes, thereby producing spurious B -mode polarization [9, 19, 20]. Additionally, due to polarization mode-mixing, new TB and EB correlations are generated. Since the standard cosmological model is parity-even the TB and EB correlations identically vanish. Therefore the TB and EB spectra can be used to probe the miscalibration of the pixel rotation angle. Furthermore, the miscalibration angle *itself* can be quantified, then removed, resulting in an unbiased measurement of B -mode polarization. This calibration procedure is accomplished *during* data acquisition, requiring no additional observing time. Therefore it is referred to as "self-calibration". Moreover, since the calibration signal is the CMB itself, any concerns that the detector response will behave nonlinearly are eliminated.

It has been shown that miscalibration produces a distinct signature in the (otherwise zero) $\langle EB \rangle$ and $\langle TB \rangle$ correlations. The amplitude of these "forbidden" correlations is proportional to the amount of miscalibration and, furthermore, it is known that several other instrumental systematics can be detected using these EB and TB correlations [18, 20]. This paper uses these correlations to calibrate CMB polarimeters to levels not achievable with laboratory or astrophysical sources.

Polarization Map Making and Miscalibration: Following [6], the timestream data from a single polarization sensitive detector, d_i , is written as

$$d_i = g_i [T(\mathbf{p}) + \gamma_i(Q(\mathbf{p}) \cos 2\psi_i + U(\mathbf{p}) \sin 2\psi_i)], \quad (1)$$

where g_i is the flux calibration, or "gain" for the i -th detector, T, Q, U are the beam-integrated CMB Stokes parameters for the map pixel in direction \mathbf{p} , $\gamma_i \equiv (1 - \epsilon_i)/(1 + \epsilon_i)$ is the polarization efficiency factor, ϵ_i is the polarization leakage for the i -th detector, and ψ_i is the detector's polarization orientation projected on the sky. The goal of mapmaking is to recover T, Q, U from the detector timestreams.

The angle ψ_i is modeled as

$$\psi_i = \psi_{\text{design}} + \Delta\psi, \quad (2)$$

where ψ_{design} is the intended orientation of the detector on the sky with respect to right ascension and declination and $\Delta\psi$ is the miscalibration of the detector. Figure 1 displays the coordinate system used for a single polarization sensitive detector.

Calibration of the detector's pixel rotation is one of the most challenging tasks facing the experimentalists [11, 21]. A miscalibration of the detector's polarization angle by an amount $\Delta\psi$ rotates primordial

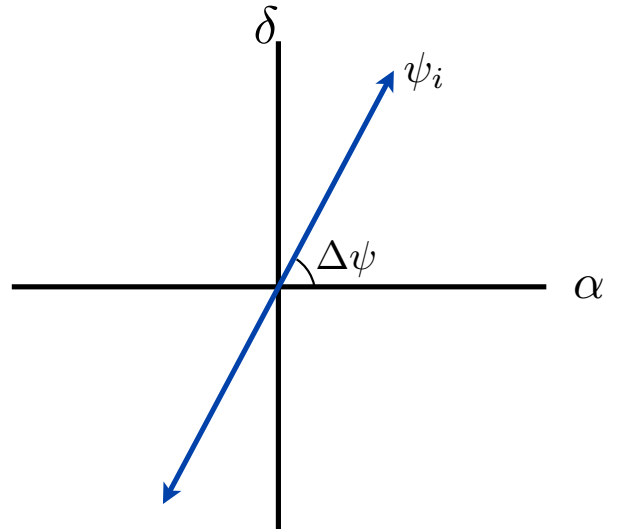


FIG. 1: Coordinate system showing the relevant angles from equation (2) for a single polarization sensitive detector. The horizontal and vertical axes are right ascension (α) and declination (δ). For this detector ψ_{design} was intended to be parallel to α .

Stokes parameters $\tilde{Q}(\mathbf{n})$, and $\tilde{U}(\mathbf{n})$ into the observed quantities:

$$Q(\mathbf{n}) \pm iU(\mathbf{n}) = e^{\pm 2i\Delta\psi}(\tilde{Q}(\mathbf{n}) \pm i\tilde{U}(\mathbf{n})). \quad (3)$$

The measured Fourier modes, $E(\mathbf{l})$ and $B(\mathbf{l})$, written in terms of the primordial modes $\tilde{E}(\mathbf{l})$ and $\tilde{B}(\mathbf{l})$, become

$$\begin{aligned} E(\mathbf{l}) &= \cos(2\Delta\psi)\tilde{E}(\mathbf{l}) + \sin(2\Delta\psi)\tilde{B}(\mathbf{l}) \\ B(\mathbf{l}) &= -\sin(2\Delta\psi)\tilde{E}(\mathbf{l}) + \cos(2\Delta\psi)\tilde{B}(\mathbf{l}). \end{aligned} \quad (4)$$

The above equations show that pixel rotation modifies the power spectra of $E(\mathbf{l})$ and $B(\mathbf{l})$ and generates spurious correlation between $E(\mathbf{l})$ and $B(\mathbf{l})$ and between $T(\mathbf{l})$ and $B(\mathbf{l})$, modifying the observed power spectra as follows:

$$\begin{aligned} C_\ell^{TE} &= \cos(2\Delta\psi)\tilde{C}_\ell^{TE} \\ C_\ell^{EE} &= \sin^2(2\Delta\psi)\tilde{C}_\ell^{BB} + \cos^2(2\Delta\psi)\tilde{C}_\ell^{EE} \\ C_\ell^{EB} &= \frac{1}{2}\sin(4\Delta\psi)(\tilde{C}_\ell^{BB} - \tilde{C}_\ell^{EE}) \\ C_\ell^{TB} &= -\sin(2\Delta\psi)\tilde{C}_\ell^{TE} \\ C_\ell^{BB} &= \cos^2(2\Delta\psi)\tilde{C}_\ell^{BB} + \sin^2(2\Delta\psi)\tilde{C}_\ell^{EE}. \end{aligned} \quad (5)$$

Here, and throughout, tildes represent primordial quantities. From Eq. 5 it is clear that pixel rotation generates spurious B -modes in the absence of primordial B -modes. Calibration of the pixel rotation involves finding $\Delta\psi$ for the detector system and removing it from the data prior to map making (Eq. 1). This procedure will recover the unrotated, primordial CMB polarization spectra.

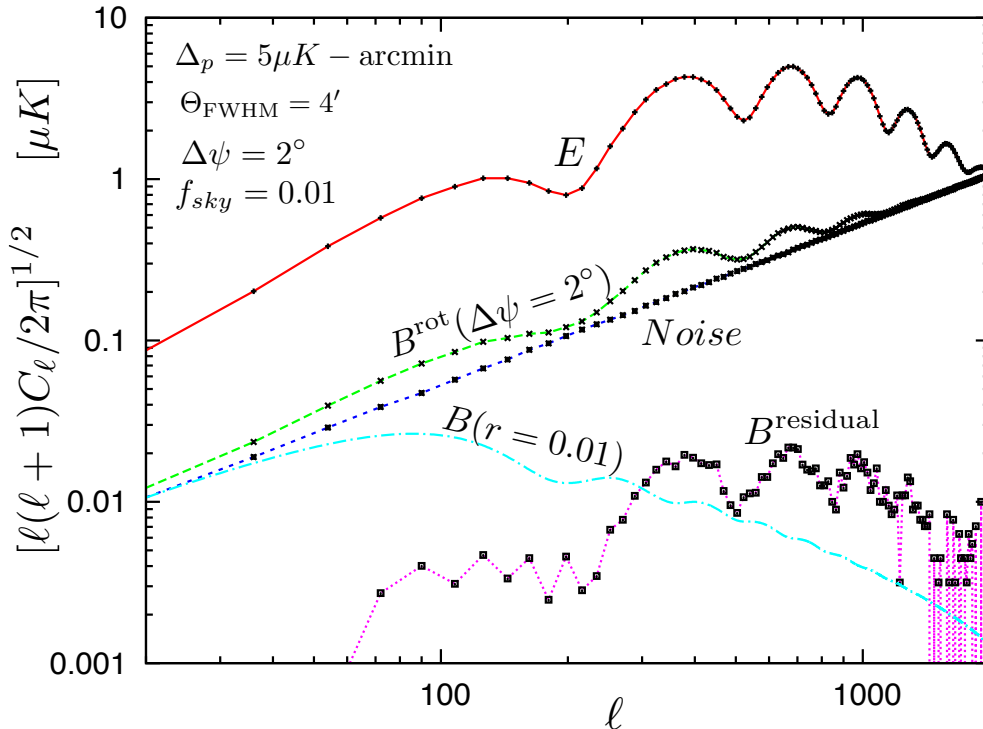


FIG. 2: Simulation demonstrating the self-calibration of pixel rotation using the CMB’s EB power spectrum. The polarization angle’s miscalibration angle is assumed to be $\Delta\psi = 2^\circ$, and the instrumental noise is $\Delta_E = \Delta_B = 5\mu K$ -arcmin. The beam’s full-width at half-maximum is $\Theta_{\text{FWHM}} = 4'$. The solid red curve shows the E -mode power spectrum, the green long-dashed curve shows the B -modes induced by miscalibration. The blue short-dashed curve shows the B -mode after correcting for the miscalibrated pixel rotation angle. Finally, to demonstrate how well the self-calibration works, the instrumental noise contribution is subtracted from the de-rotated B -mode in the bottom-most (magenta dotted) curve; these are residual B -modes remaining after self-calibrating the instrument. The primordial B -mode spectrum corresponding to $r = 0.01$ is shown in dot-dashed (cyan) line. For clarity, the lensing B -modes are omitted.

In the absence of cosmological parity violation leading to cosmic birefringence [22, 23], the detection of EB and TB spectra – each having the *same* implied pixel rotation angle $\Delta\psi$ – directly implies that the detector’s polarization angles have been miscalibrated. Such miscalibration can be caused, *e.g.*, by fabrication errors or sources of birefringence in the telescope’s optics.

The miscalibration angle $\Delta\psi$, is obtained from the observed C_ℓ^{TB} and C_ℓ^{EB} by minimizing the variance of the difference between the observed and theoretical power power spectra as a function of $\Delta\psi$.

Using Eq. 5, the two independent likelihood functions for the miscalibrated pixel rotation angle, $\Delta\psi$, become

$$\begin{aligned} \mathcal{L}_{TB} &\propto \exp \left[- \sum_l \frac{(C_l^{TB} + \sin 2\Delta\psi \tilde{C}_l^{TE})^2}{2(\delta C_l^{TB})^2} \right] \\ \mathcal{L}_{EB} &\propto \exp \left[- \sum_l \frac{(C_l^{EB} + \frac{1}{2} \sin 4\Delta\psi \tilde{C}_l^{EE})^2}{2(\delta C_l^{EB})^2} \right]. \end{aligned} \quad (6)$$

For simplicity, in Eq. 6 it is assumed that $\tilde{C}_l^{EE} \gg \tilde{C}_l^{BB}$, and that

$$\begin{aligned} (\delta C_\ell^{TB})^2 &= \frac{1}{(2\ell+1)f_{\text{sky}}} C_\ell^{TT,\text{tot}} C_\ell^{BB,\text{tot}} \\ (\delta C_\ell^{EB})^2 &= \frac{1}{(2\ell+1)f_{\text{sky}}} C_\ell^{EE,\text{tot}} C_\ell^{BB,\text{tot}} \end{aligned} \quad (7)$$

where f_{sky} is the fraction of the sky observed, $X, Y \in \{T, E, B\}$, and

$$C_\ell^{XY,\text{tot}} = \tilde{C}_\ell^{XY} + \delta^{XY} \Delta_X^2 e^{\ell^2 \Theta_{\text{FWHM}}^2 / (8 \ln 2)}. \quad (8)$$

Here, Δ_X is the detector noise and Θ_{FWHM} is the full-width at half-maximum (FWHM) resolution of the polarimeter’s Gaussian beam.

The best-fit estimates for the pixel rotation angle are obtained by maximizing the likelihood functions,

Eq. 6, resulting in

$$\begin{aligned}\Delta\psi_{TB} &= -\frac{1}{2}\sin^{-1}\left(\frac{A_{TB}}{B_{TB}}\right) \\ \Delta\psi_{EB} &= -\frac{1}{4}\sin^{-1}\left(\frac{2A_{EB}}{B_{EB}}\right)\end{aligned}\quad (9)$$

where

$$\begin{aligned}A_{TB} &= \sum_l \frac{2\ell+1}{2} \frac{C_\ell^{TB}C_\ell^{TE}}{C_\ell^{TT,tot}C_\ell^{BB,tot}} \\ B_{TB} &= \sum_l \frac{2\ell+1}{2} \frac{(C_\ell^{TE})^2}{C_\ell^{TT,tot}C_\ell^{BB,tot}} \\ A_{EB} &= \sum_l \frac{2\ell+1}{2} \frac{C_\ell^{EB}C_\ell^{EE}}{C_\ell^{EE,tot}C_\ell^{BB,tot}} \\ B_{EB} &= \sum_l \frac{2\ell+1}{2} \frac{(C_\ell^{EE})^2}{C_\ell^{EE,tot}C_\ell^{BB,tot}},\end{aligned}\quad (10)$$

and $X \in \{T, E, B\}$.

The values for $\Delta\psi_{EB}$ and $\Delta\psi_{TB}$ obtained from observations, Eqns. 9, should agree to within the statistical uncertainty (which is derived next). The consistency $\Delta\psi_{TB} \simeq \Delta\psi_{EB}$ provides a powerful cross-check on the hypothesis that the pixel rotation has been miscalibrated. Since there is intrinsic correlation between EB and TB , for real data Eqns. 6 should be replaced with a single likelihood function that *simultaneously* uses C^{TB} , C^{EB} and their correlation, to infer a single $\Delta\psi$ value. In practice, $\Delta\psi_{EB}$ will be superior to $\Delta\psi_{TB}$ but the value of having two independent estimates, which must agree in order to apply the self-calibration method, motivates the construction of both estimators.

The signal-to-noise for the EB and TB detection is

$$\begin{aligned}\left(\frac{S}{N}\right)_{TB}^2 &= f_{sky} \sum \frac{2\ell+1}{2} \frac{(C_\ell^{TB})^2}{C_\ell^{TT,tot}C_\ell^{BB,tot}} \\ \left(\frac{S}{N}\right)_{EB}^2 &= f_{sky} \sum \frac{2\ell+1}{2} \frac{(C_\ell^{EB})^2}{C_\ell^{EE,tot}C_\ell^{BB,tot}}\end{aligned}\quad (11)$$

where f_{sky} is the fraction of the sky observed. The uncertainties in $\Delta\psi_{EB}$ and $\Delta\psi_{TB}$ are

$$\begin{aligned}\sigma_{\Delta\psi_{TB}}^2 &= \left[4f_{sky} \sum \frac{2\ell+1}{2} \frac{(\tilde{C}_\ell^{TE})^2}{\tilde{C}_\ell^{TT,tot}\tilde{C}_\ell^{BB,tot}}\right]^{-1} \\ \sigma_{\Delta\psi_{EB}}^2 &= \left[4f_{sky} \sum \frac{2\ell+1}{2} \frac{(\tilde{C}_\ell^{EE} - \tilde{C}_\ell^{BB})^2}{\tilde{C}_\ell^{EE,tot}\tilde{C}_\ell^{BB,tot}}\right]^{-1}.\end{aligned}\quad (12)$$

Equations 9 and 12 give the miscalibration of pixel rotation and its uncertainty. Armed with these quantities, the experimentalist can go back and correct the assumed polarization angle by subtracting $\Delta\psi$ from

ψ_i in Eq. 1. For a toy experiment with $\Delta_p = 5\mu K$ -arcmin, $f_{sky} = 0.01$, and $\Theta_{FWHM} = 4'$ a pixel rotation as small as $\Delta\psi \sim 0.05^\circ (3')$ can be detected using the EB power spectrum alone, and $\Delta\psi \sim 0.1^\circ$, using the TB power spectrum alone. These values are more than sufficient to detect $r = 0.01$ with $\lesssim 0.1\sigma_r$ bias. Fig. 2 shows the pixel rotation calibration method derived using the EB spectrum. A similar result can be obtained for $\Delta\psi_{TB}$.

Discussion: While pixel rotation is potentially the most pernicious obstacle to detecting primordial B-modes, there are other systematic effects such as differential ellipticity and differential pointing that can produce TB and EB correlations [18, 20]. However the TB and EB correlations induced by these systematic effects have different angular dependencies from pixel rotation [24]. Therefore, high-sensitivity observations covering large numbers of multipoles can make detailed measurements of the TB and EB correlations to quantify, and correct for these types of systematic errors. Furthermore, due to the dependence on the beamsize, for a fixed level of instrument noise, a higher resolution experiment will always calibrate pixel rotation more precisely than a lower resolution experiment.

Pixel rotation and cosmological birefringence are fully degenerate effects; *i.e.* the angle $\Delta\psi$ in Eq. (2) *could be* the sum of the two effects. However, for the purpose of B-mode detection it does not matter what causes the polarization rotation $\Delta\psi$; we simply derotate the polarization by the angle $\Delta\psi$ inferred from the EB and TB estimators. Furthermore cosmic birefringence detection is not sacrificed when cosmic birefringence is spatially varying [20, 24–28].

Complications arising from the $E - B$ separation due to partial sky coverage and the EB and TB correlations induced by gravitational lensing of the CMB by large scale structure are irrelevant to the self-calibration procedure proposed here because these EB and TB correlations couple only different ℓ -values, *i.e.*, $\langle E_\ell B_{\ell'} \rangle$ and $\langle T_\ell B_{\ell'} \rangle$ will be non-vanishing only when $\ell \neq \ell'$.

Acknowledgments: MS' work was supported by the UCSD-Tel Aviv University Cosmology Program. We thank Bryan Steinbach, Chang Feng, Zigmund Kermish, and Kam Arnold for useful comments.

-
- [1] D. Baumann et al. (CMBPol Study Team), AIP Conf. Proc. **1141**, 10 (2009), astro-ph/0811.3919.
 - [2] U. Seljak and M. Zaldarriaga, Phys. Rev. Lett. **78**, 2054 (1997).
 - [3] M. Kamionkowski, A. Kosowsky, and A. Stebbins, Phys. Rev. D **55**, 7368 (1997).
 - [4] M. Kamionkowski, A. Kosowsky, and A. Stebbins, Phys. Rev. Lett. **78**, 2058 (1997).

- [5] K. T. Story, C. L. Reichardt, Z. Hou, R. Keisler, K. A. Aird, B. A. Benson, L. E. Bleem, J. E. Carlstrom, C. L. Chang, H. Cho, et al., ArXiv e-prints (2012), astro-ph/1210.7231.
- [6] H. C. Chiang, P. A. R. Ade, D. Barkats, J. O. Battle, E. M. Bierman, J. J. Bock, C. D. Dowell, L. Duband, E. F. Hivon, W. L. Holzapfel, et al., *Astrophys. J.* **711**, 1123 (2010), astro-ph/0906.1181.
- [7] R. Hlozek, J. Dunkley, G. Addison, J. W. Appel, J. R. Bond, C. Sofia Carvalho, S. Das, M. J. Devlin, R. Dünner, T. Essinger-Hileman, et al., *Astrophys. J.* **749**, 90 (2012), astro-ph/1105.4887.
- [8] E. Komatsu, K. M. Smith, J. Dunkley, C. L. Bennett, B. Gold, G. Hinshaw, N. Jarosik, D. Larson, M. R. Nolta, L. Page, et al., *Astrophysical Journal Suppl.* **192**, 18 (2011), astro-ph/1001.4538.
- [9] W. Hu, M. M. Hedman, and M. Zaldarriaga, *Phys. Rev. D* **67**, 043004 (2003).
- [10] B. G. Keating, C. W. O’Dell, J. O. Gundersen, L. Piccirillo, N. C. Stebor, and P. T. Timbie, *Astrophysical Journal Supplement* **144**, 1 (2003), arXiv:astro-ph/0111276.
- [11] Y. D. Takahashi, P. A. R. Ade, D. Barkats, J. O. Battle, E. M. Bierman, J. J. Bock, H. C. Chiang, C. D. Dowell, L. Duband, E. F. Hivon, et al., *Astrophys. J.* **711**, 1141 (2010), astro-ph/0906.4069.
- [12] J. R. Hinderks, P. Ade, J. Bock, M. Bowden, M. L. Brown, G. Cahill, J. E. Carlstrom, P. G. Castro, S. Church, T. Culverhouse, et al., *Astrophys. J.* **692**, 1221 (2009), astro-ph/0805.1990.
- [13] O. Tajima, H. Nguyen, C. Bischoff, A. Brizius, I. Buder, and A. Kusaka, *Journal of Low Temperature Physics* **167**, 936 (2012).
- [14] J. Aumont, L. Conversi, C. Thum, H. Wiesemeyer, E. Falgarone, J. F. Macias-Perez, F. Piacentini, E. Pointecouteau, N. Ponthieu, J. L. Puget, et al., ArXiv e-prints (2009), astro-ph/0912.1751.
- [15] M. Zemcov, P. Ade, J. Bock, M. Bowden, M. L. Brown, G. Cahill, P. G. Castro, S. Church, T. Culverhouse, R. B. Friedman, et al., *Astrophys. J.* **710**, 1541 (2010), astro-ph/0908.2431.
- [16] I. Agudo, C. Thum, H. Wiesemeyer, S. N. Molina, C. Casadio, J. L. Gómez, and D. Emmanoulopoulos, *Astronomy and Astrophysics* **541**, A111 (2012), arXiv:1201.2150.
- [17] T. Matsumura, P. Ade, D. Barkats, D. Barron, J. O. Battle, E. M. Bierman, J. J. Bock, H. C. Chiang, B. P. Crill, C. D. Dowell, et al., in *Society of Photo-Optical Instrumentation Engineers (SPIE) Conference Series* (2010), vol. 7741 of *Society of Photo-Optical Instrumentation Engineers (SPIE) Conference Series*, astro-ph/1007.2874.
- [18] N. J. Miller, M. Shimon, and B. G. Keating, *Phys. Rev. D* **79**, 103002 (2009), astro-ph/0903.1116.
- [19] M. Shimon, B. Keating, N. Ponthieu, and E. Hivon, *Phys. Rev. D* **77**, 083003 (2008), astro-ph/0709.1513.
- [20] A. P. S. Yadav, M. Su, and M. Zaldarriaga, *Phys. Rev. D* **81**, 063512 (2010), astro-ph/0912.3532.
- [21] QUIET Collaboration, C. Bischoff, A. Brizius, I. Buder, Y. Chinone, K. Cleary, R. N. Dumoulin, A. Kusaka, R. Monsalve, S. K. Naess, et al., ArXiv e-prints (2012), astro-ph/1207.5562.
- [22] A. Lue, L. Wang, and M. Kamionkowski, *Phys. Rev. Lett.* **83**, 1506 (1999), arXiv:astro-ph/9812088.
- [23] S. Alexander and N. Yunes, *Phys. Repts.* **480**, 1 (2009), astro-ph/0907.2562.
- [24] A. P. S. Yadav, M. Shimon, and B. G. Keating, *Phys. Rev. D* **86**, 083002 (2012), 1207.6640.
- [25] M. Kamionkowski, ArXiv e-prints (2008), arXiv:0810.1286.
- [26] A. P. S. Yadav, R. Biswas, M. Su, and M. Zaldarriaga, *Phys. Rev. D* **79**, 123009 (2009), astro-ph/0902.4466.
- [27] V. Gluscevic, M. Kamionkowski, and A. Cooray, *Phys. Rev. D* **80**, 023510 (2009), astro-ph/0905.1687.
- [28] V. Gluscevic, D. Hanson, M. Kamionkowski, and C. M. Hirata, ArXiv e-prints (2012), astro-ph/1206.5546.